

Photoemission studies of graphite high-energy conduction-band and valence-band states using soft-x-ray synchrotron radiation excitation

A. Bianconi*

Stanford Synchrotron Radiation Project, Department of Applied Physics, Stanford University, Stanford, California 94305

S. B. M. Hagström and R. Z. Bachrach

Xerox Palo Alto Research Center, Palo Alto, California 94304

(Received 22 August 1977)

Photoemission spectra of the valence band of single-crystal graphite were measured using synchrotron radiation in the energy range 33–200 eV. For $\hbar\omega = 122$ eV, good agreement was found with the calculated density of states since the matrix elements for the p -like and s -like states are nearly the same. Using constant-initial-state spectroscopy, we have found that, for $\hbar\omega < 90$ eV, the cross section of the transitions from the π and σ initial states in the valence band to the high-energy final states is governed by the joint density of states and the selection rules. We have verified the theoretical prediction of the energy and symmetry of the conduction bands between 30 and 50 eV above the Fermi energy. For $\hbar\omega > 90$ eV, the transition cross sections are mainly determined by the atomic character of the initial states.

I. INTRODUCTION

To elucidate the electronic structure and provide an experimental basis for band-structure calculations for graphite, we have performed a series of photoemission experiments using monochromatized synchrotron radiation in the energy range 33–200 eV. Graphite is an interesting example of a layered material with only s and p ($2s^2$ and $2p^4$) electrons contributing to the valence band. This consists of weak π bonds originating from $2p_z$ orbitals between the layers along the crystallographic c axis. The strong bonding in the planes is due to occupied σ bonds from $2s$, $2p_x$, and $2p_y$ orbitals. Detailed band-structure calculations have been made for graphite¹⁻³ up to energies 50 eV above the Fermi energy. The filled-valence-band structure has previously been studied by x-ray emission spectroscopy,⁴ which gives information of the p character of the valence band due to the selection rule governing the dipole transition ($p \rightarrow s$). X-ray photoelectron spectroscopic (XPS) data⁵ enhance the s part of the band due to the high s to p cross-section ratio for the high photon energies involved in these experiments (1487 eV). Existing optical data do not give information on the whole part of the band due to the large bandwidth.

There are several mechanisms which will cause structure changes in the photoemission spectra with varying excitation energy. Two of them are important in a crystal like graphite where strong selection rules are active and for high excitation energies. First, excitations to final-state energies still in the band-structure region are gov-

erned by the joint density of states and by symmetry selection rules. For polarized light with the \vec{E} vector parallel to the crystal c axis ($\vec{E} \parallel \vec{c}$), only transitions changing the parity sign ($\sigma \rightleftharpoons \pi$) are allowed, while for $\vec{E} \perp \vec{c}$ only $\sigma \rightarrow \sigma$ and $\pi \rightarrow \pi$ transitions are allowed. These selection rules are strictly valid for an ideal two-dimensional system. Graphite is a good approximation of such a system. If the symmetry of the initial-state energy is known, it is thus feasible to obtain information on the symmetry of the conduction-band final state by comparing the partial cross sections of the initial states for varying excitation energies and polarization directions. Second, for higher excitation energies, the observed structural changes in the photoelectron spectra can be explained as an atomic effect. The final-state wave function can be well approximated by a plane wave and the energy dependence of the initial-state partial cross section is characteristic of the s or p atomic-symmetry character of the initial states. We have found that for photon energies lower than approximately 90 eV, the final state should be considered a crystal state defined by band theory. Above this, the electron energy is high enough so that the free-electron approximation can be considered good. Below ≈ 90 eV the first mechanism largely determines the variation of the photoelectron energy distribution curves (EDC) with the excitation energy. The photoelectron spectra in this energy region have yielded detailed information on the high-energy electron band states of the crystal. Above ≈ 90 eV, the second mechanism predominates and it has been possible to record the increase of the partial cross section of the s -

like initial states relative to that of the p -like initial states.

II. EXPERIMENTAL

The measurements reported in this work used graphite single crystals cleaved *in situ* in an ultrahigh vacuum chamber. The purity of the surface was checked with Auger electron spectroscopy. The cleavage plane was normal to the crystallographic c axis. The experiments were performed at the Stanford Synchrotron Radiation Laboratory (SSRL) using the 4° beam line with the "grasshopper" monochromator.⁶ The synchrotron radiation was monochromatized in the range 32–600 eV and focused on the sample surface. The angle of incidence for the light was 75° and the plane of incidence was horizontal (p polarization). The synchrotron radiation was highly polarized, and all the measurements were done in the condition $\vec{E} \parallel \vec{c}$, i.e., with the photon electric field \vec{E} parallel to the c axis of the sample.

The photoelectron cross section for the valence band decreases rapidly for photon energies above 150 eV. For this reason our measurements were limited to energies less than 200 eV. The photoelectron energy spectra were recorded with a double pass cylindrical mirror analyzer. The constant-initial-state spectra were taken scanning the photon energy $\hbar\omega$ and selecting only photoelectrons

with kinetic energy $E_k = \hbar\omega - E_i$, where E_i is the binding energy of the initial state below the vacuum level E_v . The data acquisition and handling were done by a computer (PDP 11/40) connected on line.

The photoelectron energy spectra were recorded at a pass energy E_p of the cylindrical mirror analyzer (CMA) of 25 eV. The constant initial state spectra were recorded with $E_p = 50$ eV. The resolution is related to the pass energy by the formula $\Delta E = 0.016 E_p$. This gives us a resolution $\Delta E = 0.4$ eV for the EDC's since the monochromator contribution is smaller for the applied photon energies.

The constant initial state spectra (CIS) should be corrected for the transmission of the CMA. The transmitted current is theoretically given by $I \approx E_p/E_k$.⁷ We have corrected the raw data using the above formula but it should be remembered that the transmitted current goes as $I = (E_p/E_k)^n$, where n is larger than 1 and less than 1.5. To normalize the CIS spectra, the incoming photon flux has been measured using a photomultiplier with a sodium-salicylate converter.

III. RESULTS AND DISCUSSION

A. Valence band

Figure 1 shows the photoelectron spectra of the valence band for photon energies between 34 and 200 eV. It is obvious that the structure, both in the details and in the gross features, is strongly dependent on the excitation energy. For identification purposes, we have arbitrarily assigned letters to the different features. For the low photon energies, the valence-band part of the spectrum rides on a sloping background of secondaries. At the high photon energies, however, the valence band stands out clearly enough to enable an accurate assignment of the total bandwidth which we measure to be 22.5 eV. Band-structure calculations give a width of 20.5 eV.³

By comparison with the most recent band calculation using the discrete variational method,³ good agreement was found between the energy of the critical points in the valence band and the peaks in the photoemission spectrum. No surface states are expected or have been measured in graphite whose bulk electronic structure is well approximated by the electronic structure of one monolayer.¹

Figure 2 shows the theoretical band structure of graphite calculated by Painter.³ The dashed lines are bands of π symmetry and the solid lines are σ bands. The subscript v distinguishes the bands below the Fermi energy E_F .

The small peak A in Fig. 1 can be assigned to critical point K_1^- in the \vec{k} direction, which is at

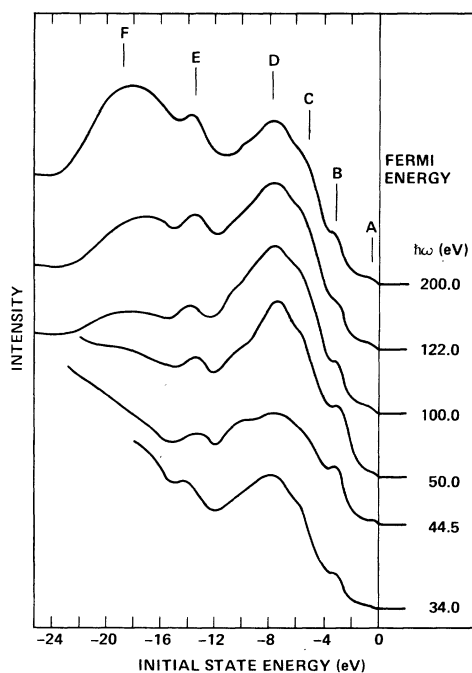


FIG. 1. Photoelectron spectra with variable excitation energy of the graphite valence band.

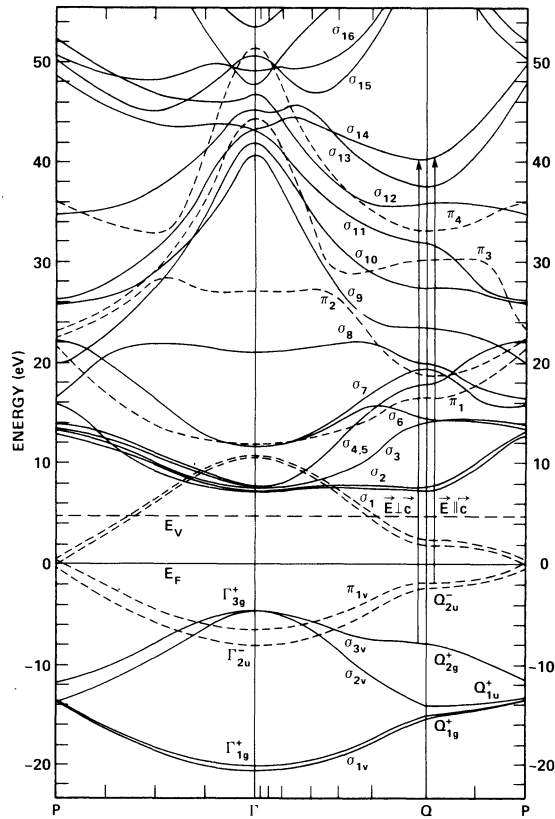


FIG. 2. Calculated valence and conduction bands of graphite (Ref. 3). E_F is the Fermi energy and E_v is the vacuum level 4.7 eV above E_F . The dashed lines are π bands and the solid lines are σ bands. The subscript v indicates the bands below E_F . The arrows indicate transitions at the same final-state energies allowed respectively for $\vec{E} \parallel \vec{c}$ and for $\vec{E} \perp \vec{c}$.

0.5 eV below the Fermi energy.⁸ Structure *B* is related to the critical point Q_{2u}^- of the π_{1v} band which is formed by $2P_z$ orbitals. Peak *C* corresponds to the crossing of the π_{1v} and σ_{3v} bands at Γ^1 . We believe that the Q_{2g}^+ critical point of the σ_{3v} band contributes mostly to the *D* peak.⁹ This band is mostly p like since it is contributing to the strongest peak in the $K\alpha$ soft-x-ray emission spectrum.^{4,10} Peak *E* is due to the high density of states near the critical point Q_{1u}^+ of the σ_{2v} which is formed by $2s$, $2p_x$, $2p_y$ orbitals. Structure *F* corresponds to the broad density-of-states maximums above Γ_{1g}^+ which is mostly s like. This band is the main peak in the x-ray photoemission spectra (XPS) of graphite.^{5,11} XPS spectra have the s -like part of the spectrum enhanced relative to those taken at low energies. The relative cross section for carbon $2s$ and $2p$ electrons is $\Sigma_{2s}/\Sigma_{2p} = 13$ for $\hbar\omega = 1487$ eV.¹²

In Table I are listed the energies of the experi-

TABLE I. Tentative assignment of the symmetry points in the graphite valence band corresponding to the experimental structures.

Peaks	Energy below E_F (eV)	Symmetry point	Band
A	0.7	K_1^-	π_{1v}
B	3	Q_{2u}^-	π_{1v}
C	5.7	$\Gamma_{3g}^+, \Gamma_{2u}^-$	π_{1v}, σ_{3v}
D	8	Q_{2g}^+	σ_{3v}
E	13.6	Q_{1u}^+	σ_{2v}
F	≈ 19		σ_{1v}
Bottom of the valence band	22.5	Γ_{1g}^+	σ_{1v}

mental structures and the assigned theoretical valence-band features. The XPS measurements of the total bandwidth gave¹¹ 30 eV and 24 eV,⁵ in contrast with the theoretical calculations,¹⁻³ 19.3 (Ref. 2) or 20.5.³ Our value of 22.5 is closer to the Painter calculation of 20.5 eV. We have observed that impurities on the surface of samples not cleaved in ultrahigh vacuum produce an increase of the strength of the *F* peak at the bottom of the valence band and the bottom of the valence band becomes broader and goes to higher binding energy. This can explain the high values of the bandwidth found in the other experiments.

At 122 eV photon energy, as will be discussed in Sec. III B, the ratio of the $2s$ and $2p$ photoemission cross section is nearly 1, so the matrix element does not affect the measured experimental photoelectron spectrum, and it is a direct mea-

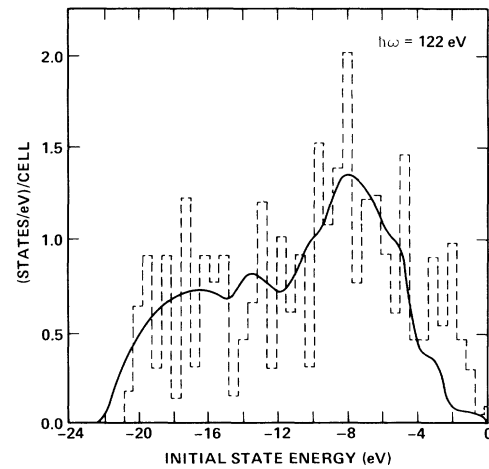


FIG. 3. Photoelectron energy distribution curve at $\hbar\omega = 122$ eV including the inelastic background subtraction. The dashed curve is the theoretical density of states.

surement of the density of states of the initial states. The photoelectron spectrum of the valence band for $\hbar\omega = 122$ eV is plotted in Fig. 3 with the inelastic background subtracted and with the one-electron density of states calculated by Painter.³ The agreement is quite good, showing that our measurements directly reflect the valence band density of states that was impossible to obtain directly by other spectroscopies such as ultraviolet photoemission spectroscopy (UPS), x-ray photoelectron spectroscopy (XPS), and x-ray emission spectroscopy.

B. High-energy states

Constant-initial-state spectra (CIS) are shown in Fig. 4 for three initial states. The initial states at Q_{2u}^- corresponding to the peak B and at Q_{2g}^+ corresponding to the peak D are both *p* like and in the *Q* direction but with opposite π and σ crystal symmetry. The other state selected corresponds to peak F which is *s* like. The points in Fig. 4 are the raw data normalized to the incident photon flux. The dashed curves are the CIS spectra corrected for the transmission of the CMA.

The lack of knowledge of the exact form of the photoelectron escape depth as a function of electron kinetic energy for graphite restricts us from taking into account the contribution of the increase of the penetration depth with electron kinetic energy. This correction would decrease the intensity of the spectra at high energies. In addition, the incident-photon flux was measured with a detector which has an increasing but unknown efficiency for increasing photon energies. At low energies the contribution from the secondaries has to be considered. In addition to these difficulties in obtaining the actual initial state cross sections from the CIS spectra, the energy dependence of the electron-electron scattering cross section can modulate the CIS. In fact we have observed that the plasmon loss of the 1s core photoelectron peak has a threshold.¹³ Only photoelectrons with kinetic energy greater than ≈ 100 eV show a measurable plasmon side band. This effect should produce a

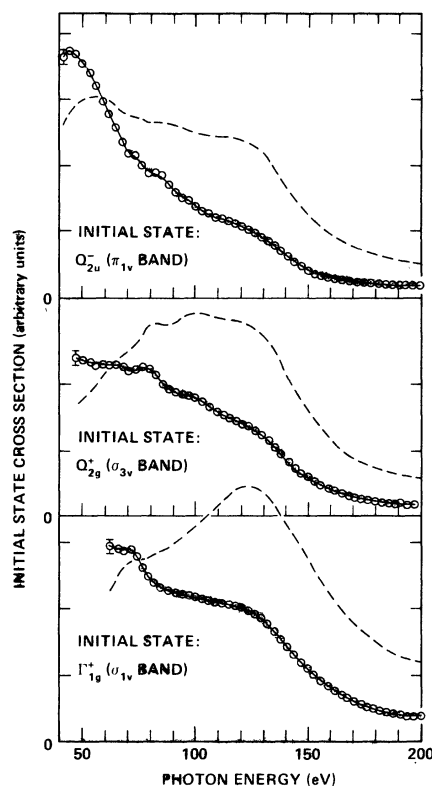


FIG. 4. Constant-initial-state spectra. The open circles are the raw data. The dashed curves include the correction for the collecting efficiency of the cylindrical mirror analyzer.

decrease of the intensity of the CIS spectra at about 100 eV due to the onset of the plasmon inelastic scattering of the direct photoemitted electrons. For all these reasons the CIS spectra are only a qualitative measurement of the partial cross section of the selected initial state. To overcome these difficulties we have measured the ratio of CIS spectra of two initial states at the same final state energy, so that all the discussed corrections are eliminated.

In Table II the energies of the structures in the constant initial state spectra are shown. Assum-

TABLE II. Structures in the constant-initial-state spectra.

Critical point (eV)	Initial state		$\hbar\omega$ (eV)	Structures Final state energy above E_F
	Band	Atomic symmetry		
Q_{2u}^-	π_{1v}	<i>p</i> like	43	40
			52	45
			72	65
			85	82
Q_{2g}^+ above Γ_{1g}^+	σ_{3v}	<i>p</i> like	76	68
	σ_{1v}	<i>s</i> like	72	53

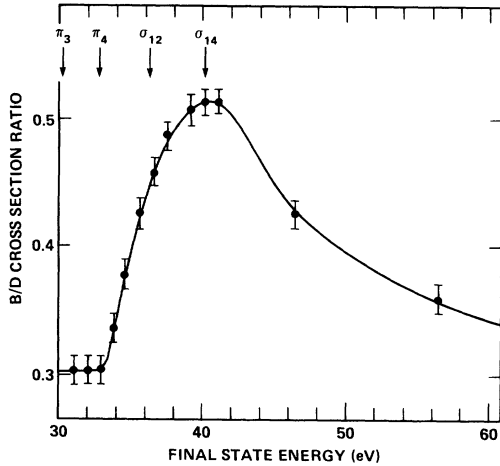


FIG. 5. Ratio of the partial photoemission cross sections from initial state π (feature B of EDC) and σ (feature D of EDC) at the same final-state energy. The arrows indicate the calculated final-state band.

ing the direct k -conserving transition model, these spectra are determined by the joint density of states and the strong selection rules which govern the interband transitions in a strongly anisotropic material such as graphite. Since we are using photons polarized with $\vec{E} \parallel \vec{c}$, only $\pi \rightarrow \sigma$ or $\sigma \rightarrow \pi$ transitions are allowed.

To obtain an experimental verification of the energy position and the symmetry of the conduction bands between 30 and 50 eV shown in Fig. 2, we have plotted the ratio of the photoemission cross sections for transitions to the same final state from two initial states with opposite crystal symmetry. We have selected the two initial states along the \vec{Q} direction, $Q_{2u}^-(\pi)$ and $Q_{2g}^+(\sigma)$, separated by 5 eV. In Fig. 5 we have plotted the ratio of the partial photoemission cross sections $\Sigma_{Q_{2u}^-(\pi)}(\hbar\omega - E_1) / \Sigma_{Q_{2g}^+(\sigma)}(\hbar\omega' - E_2)$, where E_1 and E_2 are the initial-state energies below the Fermi level and $\hbar\omega - E_1 = \hbar\omega' - E_2$ is the final-state energy. Since we are measuring the ratio of $(\pi \rightarrow F)/(\sigma \rightarrow F)$ transitions we will get a maximum if the final state F has a σ symmetry and a minimum if it has π symmetry. In Fig. 2 the arrows indicate the transitions that we are considering to a final state at 40 eV above the Fermi energy. The arrows in Fig. 5 indicate the energy of the π and σ bands crossing the \vec{Q} direction. Good agreement with the band-structure calculations using the variational approach has been found. A minimum has been found corresponding to the π_3 and π_4 bands crossing the \vec{Q} direction at 29 and 32 eV above E_F . A maximum arises for the final state in the σ_{14} band at 40 eV. At 40.7 eV a peak both in the secondary-electron emission spectroscopy and in the theoretical conduction-band density of states was found.³

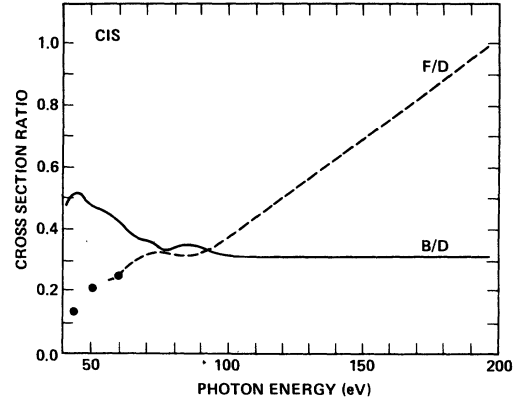


FIG. 6. Ratio of the constant-initial-state spectra from p -like states (features D and B of EDC) and s -like states (feature F of EDC) in the valence band. See Table I and Fig. 2 to identify the initial states. The points are the measure of the cross-section ratio obtained directly from the photoelectron spectra.

In Fig. 6 the ratios of the constant initial state spectra with initial states corresponding to peaks B , D , and F in the photoelectron spectra of the valence band are plotted. The solid curve is the ratio of the partial photoemission cross section of initial states with different crystal symmetry (π/σ) but both originating from the $2p$ atomic orbitals. The ratio is constant above 90 eV. This is experimental evidence that above 90 eV the photoemission cross section should be considered characteristic of the atomic wave functions which form the initial state. Moreover, the conduction bands above this energy can be considered free electron like. The dashed curve is the ratio of the photoemission cross sections of the s -like initial state corresponding to the peak F of the photoelectron spectra and the p -like initial state corresponding to the peak D . Again, for $\hbar\omega > 90$ eV no structures are observed, and a monotonic increase is measured. It is well known that in the UPS spectra the cross section of the p -like states is much higher than the cross section for the s -like states and the inverse occurs in the XPS spectra. At $\hbar\omega = 1487$ eV the ratio of the $2s$ and $2p$ carbon atomic cross sections is 13.¹² At 122 eV the ratio of the F and D peaks is ≈ 0.5 , which is close to the ratio of the theoretical density of initial states,³ so we believe that the $2s$ to $2p$ cross section ratio is close to 1 at this energy.

IV. CONCLUSION

We have obtained experimental data using synchrotron radiation-induced photoelectron spectroscopy to support theoretical calculations of the high-energy band structure of graphite by locating

the position and the symmetry of the bands between 30 and 50 eV above the Fermi energy. Using the secondary electron emission spectroscopy, it was possible to measure only the density of states of the conduction band. We have established the final-state energy ≈ 90 eV above which the free-electron approximation can be considered good and below which the band structure effects are important. Above 90 eV, partial photoionization cross sections should be characteristic of the $2p$ or $2s$ atomic wave functions.

At $\hbar\omega \approx 122$ eV the $2s$ to $2p$ cross-section ratio is close to 1, and the matrix element effects do not affect the photoelectron distribution curve. It has been possible for the first time to measure directly the valence-band density of states of graphite,

and the agreement with the theoretical density of states is good.

ACKNOWLEDGMENTS

The authors are grateful to the staff of the Stanford Synchrotron Radiation Laboratory for their support during the experiment. Thanks are due to R. S. Bauer, J. C. McMenamin, M. Hecht, and H. A. Six for help with the measurements. Stimulating discussions with E. Tosatti are gratefully acknowledged. This work was partially supported by NSF Grant No. DMR-73-07692 in cooperation with the Stanford Linear Accelerator Center and the U. S. ERDA.

*Present address: Istituto di Fisica, Università di Camerino, Camerino, Italy.

¹F. Bassani and G. Pastori Parravicini, *Electronic States and Optical Transitions in Solids* (Pergamon, New York, 1975), p. 125.

²G. S. Painter and D. E. Ellis, *Phys. Rev. B* **1**, 4747 (1970).

³R. F. Willis, B. Fitton, and G. S. Painter, *Phys. Rev. B* **9**, 1926 (1974).

⁴J. Müller, K. Fezer, G. Wiech, and A. Faessler, *Phys. Lett.* **44A**, 263 (1973).

⁵F. R. McFeely, S. P. Kowalczyk, L. Ley, R. G. Cavell, R. A. Pollak, and D. A. Shirley, *Phys. Rev. B* **9**, 5268 (1974).

⁶F. C. Brown, R. Z. Bachrach, S. B. M. Hagström, N. Lien, and C. H. Pruett, in *Vacuum Ultraviolet Radia-*

tion Physics, edited by E. E. Koch, R. Haensel, and C. Kunz (Pergamon, New York, 1974), p. 785.

⁷P. W. Palmberg, *J. Electron Spectrosc.* **5**, 691 (1974).

⁸D. L. Greenway, G. Harbeke, F. Bassani, and E. Tosatti, *Phys. Rev.* **178**, 1340 (1969).

⁹E. K. Kortela and R. Manne, *J. Phys. C* **7**, 1749 (1974).

¹⁰J. E. Holiday, *Soft X-Ray Band Spectra*, edited by D. J. Fabian (Academic, New York, 1968), p. 101.

¹¹K. Hamrin, G. Johansson, U. Gelius, C. Nordling, and K. Siegbahn, *Phys. Scr.* **1**, 277 (1970).

¹²U. Gelius, *Electron Spectroscopy*, edited by D. A. Shirley (North-Holland, Amsterdam, 1972), p. 311.

¹³R. Z. Bachrach and A. Bianconi in *Proceedings of the Fifth International Conference on Vacuum Ultraviolet Physics*, Montpellier, France, 1977 (unpublished).